Setpoint temperature estimation to achieve target solvent concentrations in *S. cerevisiae* fermentations using inverse neural networks and fuzzy logic

Vinicio Moya-Almeida [a,b,*], Belén Diezma-Iglesias [b], Eva Correa-Hernando [b,**], Cristian Vaquero-Miguel [c], Natalia Alvarado-Arias [d]

[a] *Facultad de Ingeniería, Universidad de los Hemisferios (UHE), Paseo de la Universidad, 300, 170147, Quito, Ecuador*
[b] *Laboratorio de Propiedades Físicas y Técnicas Avanzadas en Agroalimentación (LPF-TAGRALIA), Escuela Técnica Superior de Ingeniería Agronómica, Alimentaria y de Biosistemas, Universidad Politécnica de Madrid, Av. Puerta de Hierro, 2-4, 28040, Madrid, Spain*
[c] *EnotecUPM, Departamento de Química y Tecnología de Los Alimentos, Escuela Técnica Superior de Ingeniería Agronómica, Alimentaria y de Biosistemas, Universidad Politécnica de Madrid, Av. Puerta de Hierro, 2-4, 28040, Madrid, Spain*
[d] *Facultad de Arquitectura y Urbanismo, Universidad UTE, Calle Rumipamba S/N y Bourgeois, Quito, Ecuador*

** Corresponding author.

Abstract

Over the years, many technical advances have been made to improve the final quality of beers by controlling the concentrations of compounds obtained at the end of alcoholic fermentation. However, these efforts have mainly focused on increasing ethanol and reducing other compounds considered defects. This study addresses the challenge of obtaining specific concentrations of four solvent compounds (*isobutanol*, *ethyl acetate*, *amyl alcohols*, and *n-propanol*) produced by the yeast *S. cerevisiae* Safale S04, determined by an expert. A model based on four inverse neural networks (INNs) has been developed to predict the target temperature required to achieve the desired concentrations. These INNs have been trained using virtual data generated by four artificial neural networks (ANNs), as described in detail in previous work. For implementation, a fuzzy control system based on the Mamdani inference method was utilized. To experimentally validate the results, four complete fermentations were conducted. The INNs were found to be accurate tools for predicting the target temperatures based on predetermined compound concentrations, with R^2 values ranging from 0.982 to 0.986. When comparing the experimental concentration data, the most accurate prediction was achieved for *n-propanol*, with an average error of 0.18 mg L^{-1}, while *ethyl acetate* had an error of 0.25 mg L^{-1}, *isobutanol* had an error of 0.48 mg L^{-1}, and *amyl alcohols*, being the least precise prediction, had an error of 0.83 mg L^{-1}.

Keywords:

Expert system, Beer quality, Beer fermentation, Inverse neural networks, *S. cerevisiae*, Fuzzy controller

Data availability

Data will be made available on request.

1 Introduction

Beer is a beverage produced by alcoholic fermentation primarily from *S. cerevisiae* or *S. pastorianus* yeasts. Among the primary and secondary compounds produced during the process, some are crucial because of their significant influence on the organoleptic characteristics of the final product, such as higher alcohols and esters (Humia et al., 2019).

In the brewing industry, the concept of alcoholic fermentation does not strictly align with the biochemical process. Brewers consider that alcoholic fermentation begins when yeast is introduced into the fermentation vessel and continues until the initiation of the maturation phase (Oliver, 2013; White and Zainasheff, 2010). From a biochemical standpoint, this corresponds to a shorter period that encompasses glycolysis and culminates in the production of ethanol (Nelson et al., 2021). Nonetheless, in this study, we adhere to the definition provided by brewers.

The impact of these compounds is directly linked to their concentration in the final product. Therefore, the organoleptic characteristics could vary from pleasing to unpleasant (BJCP, 2015; BJCP, 2021a; Meilgaard et al., 1979). This is the principal reason why it is interesting to predict and control the concentration beforehand.

Research efforts have focused on the prediction, control, maximization or minimization of the most important compounds in beer, such as ethanol, diacetyl, or dimethyl sulfide (Carrillo-Ureta et al., 2001; Li et al., 2011; Zhang, R., 2018). As a consequence, fewer studies are found concerning secondary compounds, even though they contribute to the final organoleptic profile of beers, being pleasant at specific concentrations, as well as providing complexity, richness, and depth. The case of the ester "ethyl acetate" is known to exhibit a pleasant fruity aroma at low concentrations, while at high concentrations, it presents a pungent and unpleasant acetone-like odour (Smogrovicova and Domeny, 1999; Verstrepen et al., 2003).

The compounds selected for the experimental phase are the solvents: higher alcohols, *amyl alcohols*, *isobutanol*, *n-propanol*, and ester *ethyl acetate*. However, it does not refer to the chemical characteristics of the solvents, but rather to their organoleptic characteristics, as explained by the Beer Judge Certification Program (BJCP): "solvents: acetone-like aroma" (BJCP, 2021b).

Different studies indicate that the factors that influence the production of solvents, range from yeast genetics, wort composition, to the fermentation temperature (Loviso & Libkind, 2018, 2019), the most readily monitorable and controllable physical variable in an industrial environment.

In the literature, several studies can be found that estimate or monitor the concentrations of some secondary compounds, but we have not found any that take into consideration the organoleptic profile at the end of fermentation as a mark of product quality.

Several mathematical models for predicting alcoholic fermentation variables in beers can be found. However, the majority of these models focus on the *S. pastorianus* species, with less focus on *S. cerevisiae*. At this point, we must acknowledge a challenge inherent in the beer brewing process, namely, the high variability in raw materials, recipes, brewing processes, beer styles, and the numerous combinations that can be derived from them (Kunze and Hendel, 2019), which hinders the accuracy of mathematical models. Nevertheless, neural networks have proven to be an efficient alternative for modelling non-linear complex systems in food microbiology and fermentations, whereby by understanding the data sets of certain input and output variables, we can predict the empirical relationships between these variables (Huang et al., 2007; Syu, Tsao, Austin, Celotto, & D'Amore, 1994). With these neural networks, we can generate new artificial data sets for various purposes, such as scaling from pilot plant to industrial level or for

generating inverse neural networks, as will be explained later. Finally, it is important to consider that their implementation in embedded systems is relatively straightforward.

In this study, a group of four neural networks, developed in a previous work (Moya-Almeida et al., 2021), is utilized to estimate compound concentrations based on temperatures and times. By comparing simulated data generated by these neural networks with experimental data obtained from gas chromatography, R^2-values ranging from 0.939 to 0.996 have been achieved.

With these, artificial datasets were generated, which are reversed to train a new set of neural networks, where the outputs of the original ANNs are used as inputs for the new networks, and their inputs are treated as outputs; these novel networks are referred to, in this study, as inverse neural networks (INNs).

To the best of our knowledge, this technique has not been utilized for predicting solvent concentrations in beer fermentations to enhance the final product's quality, which constitutes one of the primary contributions of this study. Moreover, when this technique has been employed for other purposes, it typically involved incorporating a high number of inputs (measured variables). In contrast, this study prioritized a minimalist approach, employing only a direct input (temperature) along with time, thereby demonstrating the feasibility and high precision of this technique.

One of the limitations of the proposed method refers to the requirement for independent study and calculation of the data sets needed to train the initial ANNs, and the INNs, for each specific type of beer or microorganism. Therefore, it would be beneficial to develop a comprehensive database to store this information.

Subsequently, as a fermentation control tool, a controller based on fuzzy logic has been used due to its advantages, such as its simplicity, robustness, and easy practical implementation.

Fuzzy logic is an inconsistency-tolerant type of logic; that intends to go against the idea of only two possibilities as a solution to a given problem (on-off, high-low, 1-0). It recognizes that within the boundaries of these solutions, there exist intermediate points that represent diffusely the membership to a specific fuzzy set (Averill, 2020; Pedrycz, 2021; Zadeh, 1965).

Thus, a fuzzy rule defines the consequence that occurs from the relationships of two or more antecedents connected by fuzzy logical operators. Once the information enters these fuzzy rules, an inference method is needed to assess the outcome of the output variables of the consequent. One of the most used is the Mamdani method, these rules are of the IF x_1, x_2 – THEN y_{12} type. Subsequently, this conclusion is represented by an area resulting from the aggregation of all the areas produced by the evaluation of each fuzzy rule, for this reason, it is necessary to take it to a number which represents the solution that was found; this process is known as “defuzzification”. To carry out this task there are several mathematical methods, among which the centroid method stands out. (Averill, 2020; Oussalah et al., 2001).

An aspect that needs to be taken into consideration is the reliance on advanced techniques for measuring this type of compounds, such as Gas Chromatography (Martins et al., 2020; Villacreces et al., 2022), which involves sampling and sending samples to laboratories, incurring additional costs. This further emphasizes the importance of developing models for economically predicting compound concentrations, which could potentially be implemented online.

Finally, we believe that this type of system has potential applications for craft brewers, characterized by their limited purchasing power, which leads them to not implement advanced controllers but rather on-off controllers with hysteresis. For this reason, we have consistently considered that the proposed methods can be implemented on low-cost and readily accessible devices.

This study aims to showcase that the utilization of an INN in conjunction with a fuzzy logic temperature control system can effectively predict and sustain the optimal fermentation setpoint temperature to obtain the target concentrations of four solvents: *isobutanol*, *propanol*, *amyl alcohol* and *ethyl acetate*, by employing solely the temperature and its rate of change as input variables for the controller. Therefore, the goal is to develop an efficient control system with a low cost and relatively simple implementation.

The main contributions are summarized below:

- We propose a method to calculate average setpoint temperatures for obtaining expert-determined concentrations of four solvent compounds in *S. cerevisiae* fermentations.

- We have demonstrated the feasibility of calculating these setpoint temperatures through the implementation of INNs, which were trained with artificial datasets generated by ANNs trained with experimentally obtained datasets, despite the complex variability of compounds resulting from alcoholic fermentation with *S. cerevisiae*.
- The experimental results demonstrate that, at least on a pilot plant scale, temperature and its error derivative are sufficient as controlled variables, and when combined with the use of Fuzzy Control, highly accurate outcomes are achieved.
- To the best of the authors' knowledge, this is the first work that estimates parameters for bioreactor control with the ultimate goal of predicting concentrations of secondary compounds, taking into account final organoleptic quality considerations in alcoholic fermentations, based on expert knowledge.

2 Related works

In this section, a review is conducted on applications of neural networks in fermentations and fuzzy control in bioreactors.

2.1 Neural networks

Artificial Neural Networks (ANNs) have been widely used in virtually all aspects related to food sciences, and fermentations are no exception. However, as mentioned earlier, the practically infinite number of combinations of raw materials used, production methods, and microorganisms involved, results in complex, nonlinear systems with behaviours that have often been studied but are not fully understood, opening a broad spectrum of applications where neural networks have proven to be a reliable tool. The majority of these networks are of the feedforward type.

In general, artificial neural networks (ANNs) perform two types of tasks in fermentative systems. First, some directly calculate the values of the physical, chemical, or biological variables involved, such as pH, temperature, substrate quantity, etc. Second, some calculate input values or adjustments for other types of mathematical models, such as kinetics, or inputs of controllers like PIDs. (Huang et al., 2007).

For example, in the work of Zhang et al., an estimation of acetic acid concentration in beers is performed, as it is considered a quality-related issue. The authors use samples inoculated at a laboratory scale, although they do not declare the type of microorganism used. They train two ANNs, with parameters such as pitching rate, pressure, suspended cells, and generation number, among others, in addition to acetic acid concentration. (Zhang, Y., Jia and Zhang, 2013).

To predict and subsequently perform online control of biomass for yeast batch propagation in a bioreactor, Birle et al. employ a feedforward neural network with the input layer consisting of optical density, pH, and density, a hidden layer with three nodes, and an output layer that estimates yeast cell concentration. The training is conducted using the Levenberg-Marquardt backpropagation algorithm. The authors declare the use of *S. cerevisiae* sp., strain W34/70, which is indeed an *S. pastorianus*. (Birle et al., 2015).

Sipos et al. aims to estimate state variables in the alcoholic fermentation of wine with *S. oviformis* and *S. elipsoideus* at a laboratory scale. After conducting various experimental combinations, they find that the configuration that yields the best results is a Feedback neural network, with seven neurons in the input layer (temperature, time, substrate concentration, biomass, etc.), a hidden layer with twelve neurons, and alcohol concentration as the output. Finally, they use the Levenberg-Marquardt algorithm for learning. (Sipos et al., 2021).

Among other related works, we can mention the one by Medl et al., where a software sensor for optical density in high-throughput fermentations with *Escherichia coli* is developed, using a Feed-forward neural network with Leaky ReLU activation function, achieving a high level of accuracy (Medl et al., 2023).

As mentioned before, articles that consider and estimate concentrations of secondary compounds, particularly using neural networks, in beer fermentations are scarce.

2.2 Inverse neural networks

INNs technique has already been used successfully in several works. The work of (Imtiaz et al., 2013) is particularly interesting for our purpose since they work on a bioreactor that produces ethanol. The authors generate an INN, which has as outputs the estimation of temperature, pH, and dissolved oxygen, and as inputs, the input flow of a refrigerant agent, the agitation speed, and a ratio between the flows of a base and an acid. Finally, they compare the behaviour of the INN against a PID, obtaining better results for the first one due to the non-linear nature of the system; this was done as a simulation in MATLAB.

In the study conducted by (Wang, B., Ji and Zhuang, 2015), an INN is employed to overcome the challenge of directly measuring the concentrations of mycelium (X), substrate (S), and product (P) in penicillin fermentation. Other parameters such as dissolved oxygen, pH and fermentation volume can be directly measured. The three concentrations are estimated from these parameters. The researchers performed 10 fermentations, 6 to generate the database for network training, 2 for optimization, and 2 to verify the accuracy of the results. The authors highlight that better predictions of crucial process parameters were achieved, in addition to the advantage of not needing a priori-specific knowledge about penicillin fermentation.

There are other related studies, such as an application in level control in coupled tanks (Sousa et al., 2019); a decoupling control in the fermentation of marine biological enzymes (Zhu et al., 2018); and soft-sensing modelling for the penicillin fermentation process (Wang, B. et al., 2015).

2.3 Fuzzy controllers

Several works use fuzzy control as a temperature control method in alcoholic fermentation (Venkateswarlu and Gangiah, 1995; Wang, X., Liu, Song and Wu, 2015; Xu, G. & Liu, 2007; Xu, X. Q., Nov 01, 2013), furthermore (Rodrigues et al., 2013), uses it to control the final concentration of ethanol in beers, while (Martinez et al., 1999) in wine fermentation.

(Venkateswarlu and Gangiah, 1995) implement a controller using two input variables (temperature error, rate of change of temperature error) and one output (cooling). They implement two fuzzy controllers, one using four rules and the other 49, during a simulated fermentation of 150 h, which uses a kinetic model with relatively low temperatures (lager fermentation). The universe of the discourse of the proposed error is [−5, 2], which can be interpreted as more problematic when temperatures rise above the setpoint than when they fall. They conclude by comparing fuzzy controllers with conventional ones, in which they find better results in the former. They also conclude that the controller with few rules obtains similar results to the one with many rules but requires greater adjustments and precision in the fuzzy variables, even so, the results are very close.

(Xu, G. & Liu, 2007) incorporate another variable related to the temperature error change in a discrete-time to the temperature error variable. To verify the performance of the controller, a computer simulation is conducted, and to depict the system, a kinetic model is utilized. The authors mention achieving favourable control outcomes; however, they do not provide specific details regarding the universes of discourse for the variables.

(Wang, X. et al., 2015) implement a fuzzy controller, with two inputs (temperature error and rate of change of the temperature error), and three outputs corresponding to the gains Kp, Kd and Ki of a PID controller, which performs the control tasks. The universes of discourse used were [−12; 12] for the temperature error and [−0.5; 0.5] for the rate of change of the error. A simulation was conducted comparing a conventional PID controller, a fuzzy PID controller, and a variable universe fuzzy PID controller. The best results were obtained with the latter, exhibiting shorter response times, reduced peaks in the transient state, and superior performance in a steady state.

In the same work by Birle et al., mentioned earlier, the control is exerted through two fuzzy controllers, one for temperature and another for wort aeration. The temperature controller is based on two inputs: the first is the difference between the amount of biomass provided by a growth model and the estimated biomass concentration, while the second is the derivative of the former, aiming to control the rate of change. The output is the increments or decrements of temperature required by the process, which constitutes the input for a PID integrated into the PLC that controls the bioreactor. (Birle et al., 2015).

3 Materials and methods

3.1 Hardware and software

Matlab® R2021b U2 (MathWorks, Natick, MA, USA) was used for data analysis, ANNs training, fuzzy controller, and a hardware-embedded standalone application.

A Raspberry Pi 3B+ (Raspberry Pi Fdn, Cambridge, UK) was used for the implementation of the hardware-embedded standalone application. Also, it was used as a communication channel between the temperature sensor and a ThingSpeak™ channel (MathWorks, MA, USA), where the collected data was stored.

All fermentations were carried out in a 23 L stainless-steel conical fermenter with a double-walled for cooling and a heater plate for heating. To provide temperature real-time data, a Tilt™ thermometer (Tilt, CA, USA) was used inside the fermentation tank. Tilt accuracy is ±0.5 °C and the sensor sampling interval was 300 s.

3.2 Fermentation samples and analysis by GC-FID

A total of four fermentations (F1 – F4) were carried out, each fermentation lasted for a duration of ten days. Table 1 displays the target concentrations of the solvents that will be used by the INNs (R5 - R8) to calculate the setpoint temperatures to achieve these concentrations. These values were selected discretionally within the concentration ranges found by (Moya-Almeida et al., 2021), based on the asymptotic values of the functions proposed in that work. As an example, in the case of isobutanol between 16.5 and 18.0 °C of fermentation temperature, the concentration ranged from 24.58 to 36.78 mg L^{-1}, so an average concentration of 30.00 mg L^{-1} was chosen for the second fermentation (F2) of the present work; while between 18.0 and 19.0 °C, the concentration ranged from 36.78 to 42.10 mg L^{-1}, so 39.50 mg L^{-1} was chosen for F3. A similar procedure was followed for all cases (Moya-Almeida et al., 2021). These ranges were established based on the typical results obtained when *S. cerevisiae* Safale S-04 (Fermentis, Hauts-de-France, France) operates within the typical temperature ranges employed by brewers.

alt-text: Table 1

Table 1

The table layout displayed in this section is not how it will appear in the final version. The representation below is solely purposed for providing corrections to the table. To view the actual presentation of the table, please click on the Preview located at the top of the page.

Target concentrations in mg·L^{-1} of solvent compounds used as inputs for INNs R5-R8 for each fermentation.

Compounds	Fermentation 1 (F1)	Fermentation 2 (F2)	Fermentation 3 (F3)	Fermentation 4 (F4)
isobutanol	24.40	30.00	39.50	44.00
ethyl acetate	22.50	25.75	27.15	28.15
amyl alcohols	59.12	63.00	67.50	72.80
n-propanol	23.35	24.50	25.85	27.10

The standard wort produced utilizes 5.53 kg of barley malt: 90.3 % Pale Ale Golden Promise, 9 % Crystal Light and 0.7 % Crystal Extra Dark 120 °L. Mashing was carried out for 120 min at 66 °C 135 g of "EKG" type hops were used for bittering (26 % min 60, 22 % min 90, 22 % min 110, 30 % min 120), during a 2-h boiling process. *S. cerevisiae* Safale S-04 was used for main fermentation. The principal analytical characteristics of the wort are as follows: original gravity (OG) = 1.054, international bitterness unit (IBU) = 35, ABV = 5.4 %.

Starting from the initial day of fermentation, triplicate samples were collected daily to generate a dataset of 27 samples per fermentation. These samples were analyzed using gas chromatography to monitor the progression of the four solvent concentrations throughout the fermentation processes. The gas chromatograph coupled with a flame ionisation detector (GC-FID) method was described by Loira et al. as a variant of a method recommended by the International Organisation of Vine and Wine for the analysis of higher alcohols (Loira et al., 2013).

Samples were subjected to injection after being filtered through 0.45 µm polyethersulfone membrane filters (Labbox, Madrid, Spain). The gas chromatograph used in the study was the Agilent 6850 (Palo Alto, CA, USA). The injection

temperature was set at 250 °C, while the detector temperature was maintained at 300 °C. The chromatographic analysis employed a DB-624 capillary column (60 m × 250 μm × 1.40 μm) with a stationary phase consisting of 6% cyanopropyl phenyl and 94% polydimethylsiloxane. The temperature ramp for the column was initially set at 40 °C for the first 5 min, followed by a linear increase of 10 °C·min^{-1} until reaching 250 °C. The temperature was then held constant for 5 min. Each sample had a total runtime of 40 min. Hydrogen was used as the carrier gas with a flow rate of 2.2 L·min−1 through the column. Additionally, 100 μL of internal standard (4-methyl-2-pentanol, 500 mg L^{-1}) (Fluka Chemie GmbH, Buchs, Switzerland) was added to 1 mL of the test samples. The detection limit for the analysis was set at 0.1 mg L^{-1}. The volatile compounds analyzed were previously calibrated with five-point calibration curves (R^2): 1-propanol (0.999), ethyl acetate (0.999), isobutanol (0.999), 2-methyl-1-butanol (0.999) and 3-methyl-1-butanol/isoamyl alcohol (0.999).

3.3 Neural networks

In the present work, a previously described ANNs model was used (Moya-Almeida et al., 2021). Four neural networks were defined, able to predict the concentration of solvent compounds (*isobutanol* (ANN R1), *ethyl acetate* (ANN R2), *amyl alcohols* (ANN R3) and *n-propanol* (ANN R4)) as a function of fermentation temperature and time. These ANNs were used to train the new four INNs (*isobutanol* (INN R5), *ethyl acetate* (INN R6), *amyl alcohols* (INN R7) and *n-propanol* (INN R8)) (Fig. 1). Each ANN generated a dataset of 131079 points (virtual concentrations) for each solvent, plus the time scale, which were used as input for each of the four INNs. The output is the most suitable temperature to obtain an expected concentration of solvents, as defined by the user (Imtiaz et al., 2013).

alt-text: Fig. 1

Fig. 1

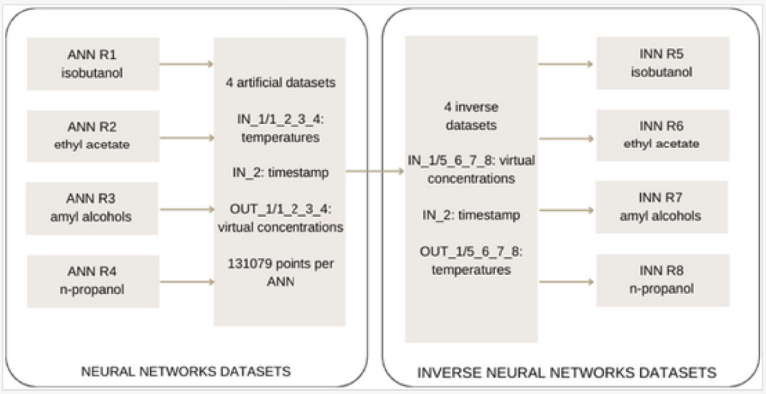

Flowchart between the artificial datasets created by the ANNs and the inverse datasets for training the INNs.

The training algorithm used was Bayesian Regularization with 50 neurons in the hidden layer for *isobutanol*, *amyl alcohols* and *n-propanol* and 90 for *ethyl acetate* (Fig. 2). In small datasets, high correlation coefficients are observed when this algorithm is applied, as (Gonzalez Viejo, Torrico, Dunshea and Fuentes, 2019) mention. Random data division was used (training: 75 % - testing: 25 %); finally, for performance purposes, Means Square Error (MSE) algorithm was used.

alt-text: Fig. 2

Fig. 2

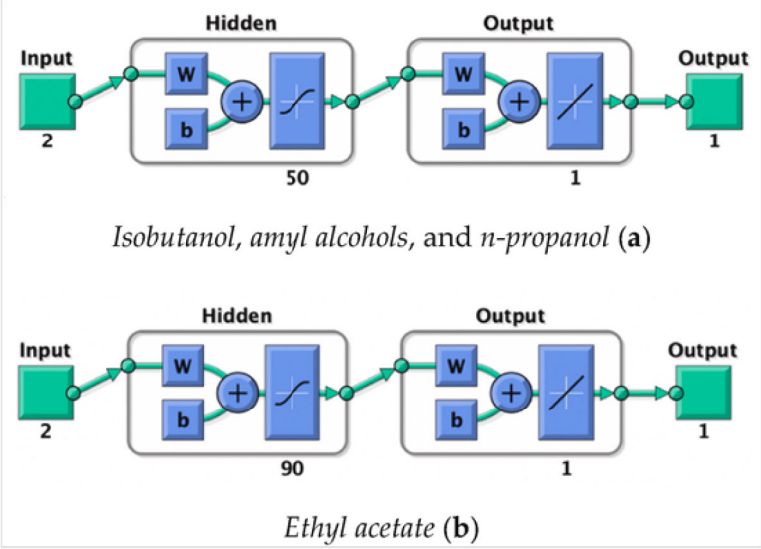

Block Diagram of the two-layer feed-forward ANNs. Linear transfer function in the output layer and tan-sigmoid function in the hidden layer was used. (a) *Isobutanol*, *amyl alcohols*, *n-propanol*, and (b) *ethyl acetate*.

The INNs predict the temperature at which the alcoholic fermentation must be carried out to obtain a specific concentration for each of the four solvents described above. The target concentrations of the studied solvents can be found in Table 1. Finally, from the four temperatures estimated by the INNs to obtain the established concentrations of each of the four compounds in the same fermentation process, the average temperature is calculated; this is the value that the controller will use as the setpoint temperature for fermentation.

The selection of parameters used for the training and configuration of the neural networks was based on similar systems found in the literature review and through continuous testing.

3.4 Fuzzy controller

The temperature determined by the INNs is utilized by an application operating with an embedded fuzzy controller (FC) to regulate a cooling pump and heating plate in a fermentation vessel. The control diagram, fuzzy inference system, and input and output variables can be seen in Fig. 3. Mamdani's method has been used as an inference method. For defuzzification, the centroid method has been selected.

alt-text: Fig. 3

Fig. 3

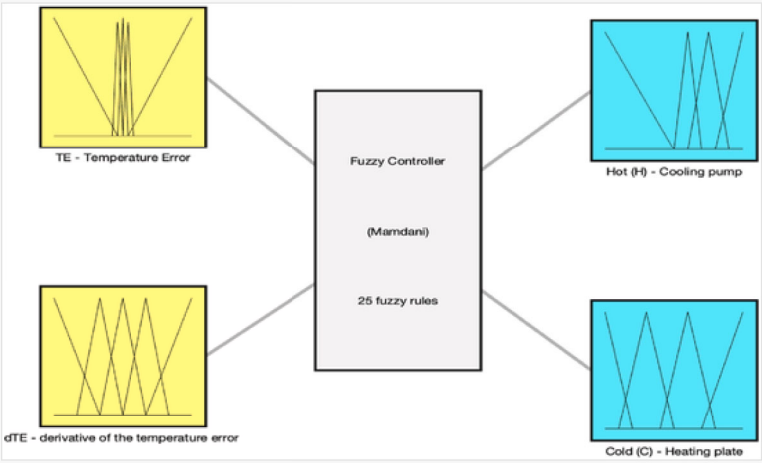

Input and output variables of the fermentation control system based on fuzzy logic with Mamdani's inference method. Temperature Error (TE), derivative of the temperature error (dTE), the wort is cold (C), the wort is hot (H).

Temperature is the primary parameter over which control is exerted, however, to avoid sudden changes in the system, the derivative of the error was incorporated, thus the linguistic variables are *temperature error* (*TE*, °C) and *derivative of the temperature error* (*dTE*, $°C \cdot s^{-1}$). TE_i represents the difference between the setpoint temperature (T_{st}) and the temperature measured by the sensor (T_i) at each time instant *i*. dTE_i represents the variation of *TE* within a sampling interval ($\Delta t = 300$ s), where TE_{i-1} represents the preceding error and TE_i represents the current error (Venkateswarlu and Gangiah, 1995). Both are described in equations (1)–(3).

$$TE_i = T_{st} - T_i \tag{1}$$

$$\frac{dTE_i}{dt} = \frac{TE_i - TE_{i-1}}{\Delta t} \tag{2}$$

$$\frac{dTE_i}{dt} = \frac{(T_{st} - T_i) - (T_{st} - T_{i-1})}{\Delta t} = \frac{T_{i-1} - T_i}{\Delta t} \tag{3}$$

The controller operates with two outputs: the first represents "wort is *cold* (*C*)" and the second represents "wort is *hot* (*H*)". Consequently, output *C* will turn on the heating plate and *H* the cooling pump.

3.5 General diagram

In Fig. 4, a general descriptive diagram of the system is depicted, showing the different levels and elements that compose it.

alt-text: Fig. 4

Fig. 4

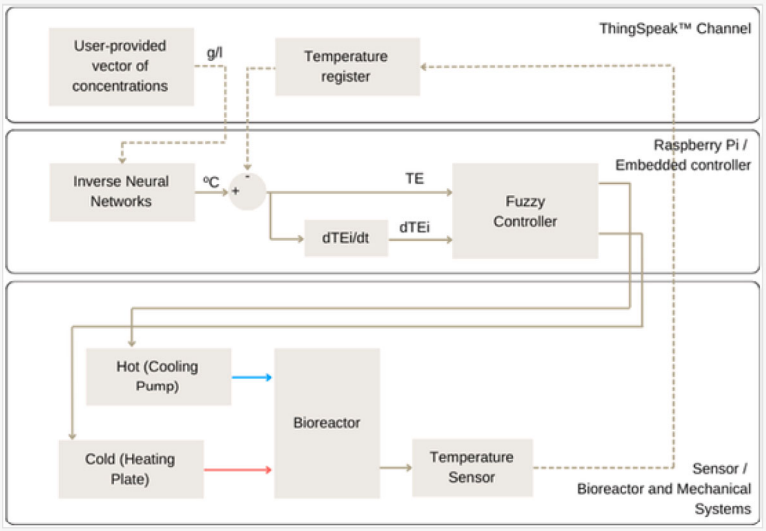

An overall diagram of the three levels of the system: the cloud subsystem (Thingspeak channel), the embedded control and prediction subsystem on the Raspberry Pi, and the bioreactor subsystem.

4 Results and discussion

4.1 Fuzzy control

As a first step, the development of the Fuzzy Controller (FC) was carried out.

The universe of discourse for the linguistic variable TE is [−4, 4] °C, which encompasses the range of values above and below the sensor measurement that the controller takes into account for implementing control functions. For *dTE,* the universe of discourse is [-6x10^{-3}, 6 × 10^{-3}] °C ·s^{-1}; which represents a maximum limit of 1.8 °C of increase or decrease in temperature every 300 s (equation (3)). As a consequence, the universe of discourse for *dTE* extends from zero to positive and negative values. Physically, positive values indicate a decreasing temperature, while negative values indicate an increasing temperature.

The parameter ranges for *TE* (0.6 °C) are calculated from the minimum resolution of the sensor (0.5 °C), in the same way, for dTE (0.002 °C·s^{-1}) it corresponds to a variation of 0.6 °C in 300 s.

Table 2 presents the detail of the fuzzy sets, subsets, discourse universes, membership functions and interpretation of all of them.

alt-text: Table 2

Table 2

The table layout displayed in this section is not how it will appear in the final version. The representation below is solely purposed for providing corrections to the table. To view the actual presentation of the table, please click on the Preview located at the top of the page.

Fuzzy sets, discourse universes, membership functions, parameters, and logical and physical interpretation.

Linguistic variables	Universes of discourse	Fuzzy subsets		Interpretation
		Membership functions	Ranges [a]	
TE: temperature error	[-4, 4] °C	VP – Very positive	[0.3, 4.0]	The wort is very cold. The measured temperature is considerably below the setpoint.
		P – Positive	[0.0, 0.6]	The wort is cold. The measured temperature is below the setpoint.
		Z – Zero	[-0.3, 0.3]	The measured temperature is within the set point or very close to it.
		N – Negative	[-0.6, 0.0]	The wort is hot. The measured temperature is above the setpoint.
		VN – Very negative	[-4.0, −0.3]	The wort is very hot. The measured temperature is considerably above the setpoint.
dTE: derivative of the temperature error	[-6x10^{-3}, 6 × 10^{-3}] °C·s^{-1}	VP – Very positive	[0.002, 0.006]	The wort is cooling very fast. The previous temperature is considerably higher than the current one.
		P – Positive	[0.0, 0.004]	The wort is cooling fast. The previous temperature is higher than the current one.
		Z – Zero	[-0.002, 0.002]	The wort is in balance. The previous temperature is similar to the current one.
		N – Negative	[-0.004, 0.0]	The wort is heating up. The previous temperature is lower than the current one.
		VN – Very negative	[-0.006, −0.002]	The wort is heating up very fast. The previous temperature is considerably lower than the current one.
C: Cold	[0, 1]	Z – Zero	[0.0,	The system is not cold or is not cooling. The heating plate

			0.2]	must not be turned on.
		L – Low	[0.1, 0.5]	The system is cold but close to the setpoint or is cooling down. The heating plate must be turned on at low power.
		M – Medium	[0.4, 0.8]	The system is cold or cooling fast. The heating plate should turn on at slightly above half power.
		H – High	[0.7, 1.0]	The system is too cold or cooling too fast. The heating plate must turn on at full power.
H: Heat	[0, 1]	Z – Zero	[0.0, 0.5]	The system is not hot or is not heating up. The cooling pump should not turn on.
		L – Low	[0.5, 0.7]	The system is hot but close to the setpoint or is heating up. The cooling pump should turn on at low power.
		M – Medium	[0.6, 0.9]	The system is hot or is heating up fast. The cooling pump should come on at slightly above half power.
		H – High	[0.8, 1.0]	The system is too hot or is heating up too fast. The cooling pump should come on at full power.

Table Footnotes

[a] All ranks are associated with the same units as their respective universes of discourse.

The detailed fuzzy sets and membership functions for the inputs and outputs can be observed in Fig. 5.

alt-text: Fig. 5

Fig. 5

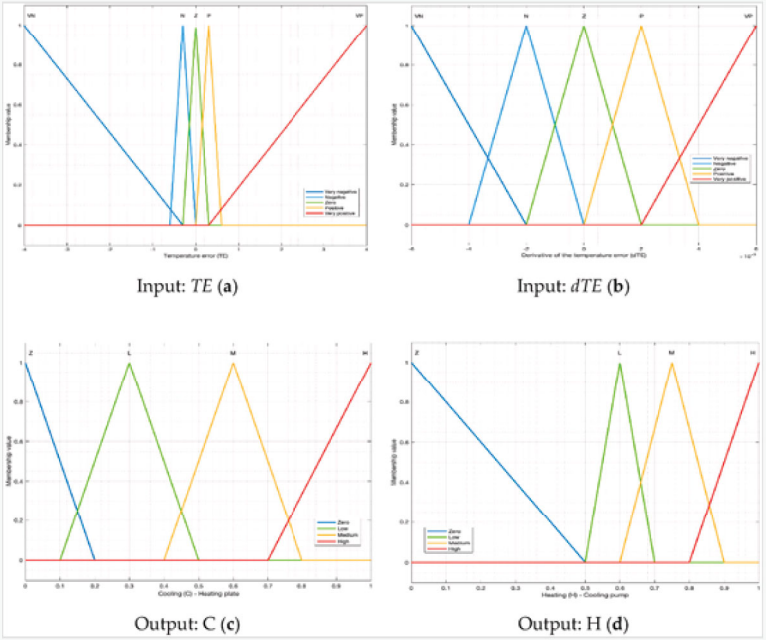

Fuzzy sets and membership functions for (a) input *temperature error*, (b) input *derivative of the temperature error*, (c) output *cold* and (d) output *heat*. Abbreviations: Very negative (VN), negative (N), zero (Z), positive (P), very positive (VP), low (L), medium (M), high (H), temperature error (TE), derivative of the temperature error (dTE), cold (C), heat (H).

The *Cold* and *Heat* membership functions have output values that are between 0 and 1; this represents the operating range (0–100 %) of the mechanisms, which are controlled with PWM (pulse width modulation) connected to optocouplers that transmit power to the heating plate and the cooling pump. It is evident, as shown in Fig. 5 (d) that the membership function of *H* is biased, the reason for restricting the membership function Z to operate from 0 to 0.5 is due to the operational challenges faced by the cooling pump when operating below 50% of its capacity.

The fuzzy rule base followed the IF-THEN structure and the Mamdani inference method was used for its aggregation. A summary of the rules can be seen in Table 2.

In the case of *TE* = N and *dTE* = VP, the wort is hot but cooling rapidly, requiring a combination of cooling and heating actions. Both outputs are in the low state (L). Due to the extensive coverage of the cooling jacket on the fermenter, the cooling process is highly efficient. To reduce the cooling rate, the heating plate, which covers only a portion of the fermenter, is slightly activated.

For example, if *TE* is between N and VN (−0.54) and the *dTE* is between Z and P (0.0014), the fuzzy control action would indicate that *Cold* is assigned a value of High level = 0.81, and *Heat* has a Zero level = 0.09. The values given to *C* and *H* are calculated from the defuzzification method, the centroid, explained above. The complete response surfaces for all the possibilities of *TE* and *dTE* can be observed in Fig. 6, where the previous example can be visually deduced.

alt-text: Fig. 6

Fig. 6

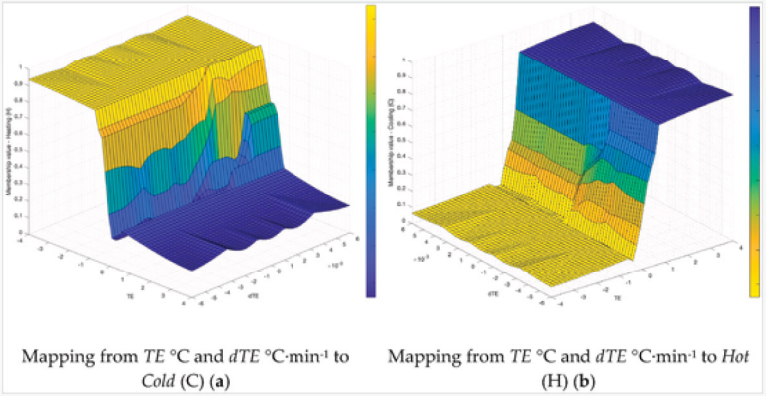

Response surfaces of fuzzy controller outputs. (a) *C*: *Cold*, (b) *H*: *Heat*. Warm colours correspond to outputs that are closer to 1, while cool colours represent outputs that are closer to 0.

4.2 INNs training

Using data simulated by ANNs R1 - R4 (inputs: time and temperature, outputs: concentrations), the four INNs R5 - R8 (inputs: time and concentrations, outputs: temperatures) were trained. For this purpose, a total of 131079 values were generated for each compound, along with two vectors of the same size: one for the variable "time" and the other for "temperature". In this manner, networks R5 - R8 carry out the inverse process to R1 - R4.

Table 3 shows the statistics that characterize the goodness of fit of the INNs R5 - R8 models. High correlation coefficients are observed, which demonstrates the high quality of the models. The worst-case mean square error is for *n-propanol* (MSE = 0.086), while the best is for *amyl alcohols* (MSE = 0.041).

alt-text: Table 3

Table 3

The table layout displayed in this section is not how it will appear in the final version. The representation below is solely purposed for providing corrections to the table. To view the actual presentation of the table, please click on the Preview located at the top of the page.

Fuzzy logic rules of the control system established by expert knowledge.

TE	dTE				
	VN	N	Z	P	VP
VP	H – Z	H – Z	H – Z	H – Z	H – Z
P	M – Z	M – Z	M – Z	H – Z	H – Z
Z	Z – L	Z – L	Z – Z	L – Z	L – Z
N	Z – M	Z – M	Z – L	Z – L	L – L
VN	Z – H	Z – H	Z – H	Z – H	Z – H

Inputs: Very negative (VN), negative (N), zero (Z), positive (P), very positive (VP). Temperature error (TE), derivative of the temperature error (dTE). Outputs: low (L), medium (M), high (H). In each pair, the first output corresponds to *Cold* and the second to *Heat*.

Fig. 7 shows, by way of example, the comparison between the temperature values simulated by R5 against the record of the temperature input of R1 for the cases of setpoint fermentation temperatures of 15 and 21 °C, described in (Moya-Almeida et al., 2021). In general, good correspondence is observed between both data sets, although there is a recurring error in the first 24 h of the experiments. As a result, the INN's algorithm strives to swiftly adjust the predicted temperature to accommodate the exponential changes in solvent concentration, particularly when the fermentation initiates at a temperature significantly distant from the setpoint (Fig. 8). To mitigate these initial disturbances in the INNs' output and accurately predict the fermentation temperature for a given solvent concentration, the controller disregards the simulated data during the first 24 h of fermentation.

Images may appear blurred during proofing as they have been optimized for fast web viewing. A high quality version will be used in the final publication. Click on the image to view the original version.

alt-text: Fig. 7

Fig. 7

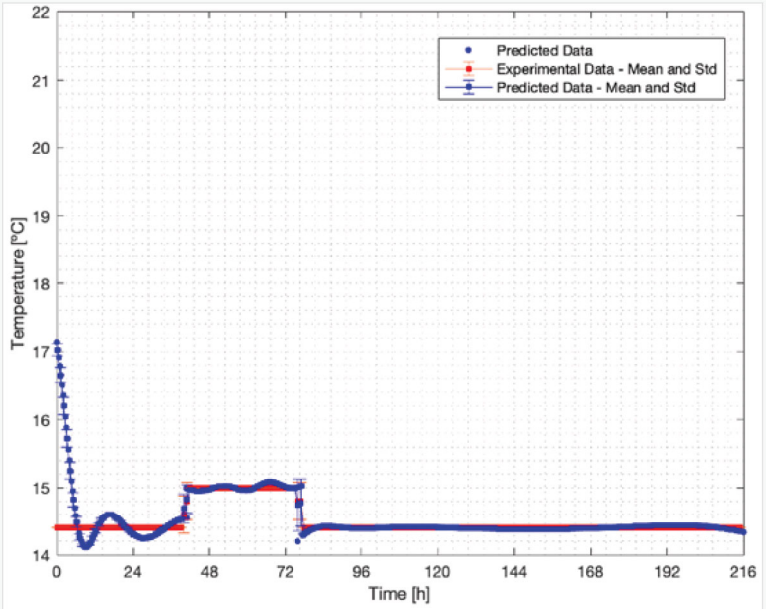

Temp 15 °C (**a**)

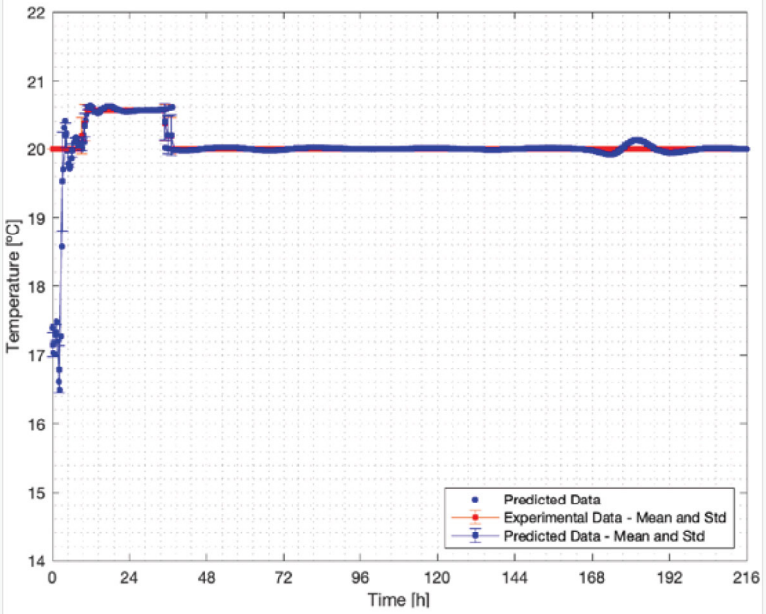

Temp 21.0 °C (**b**)

Comparative graphs of the experimental temperature values measured by the sensor (squares and red line); the temperatures predicted by the inverse neural networks (blue line), squares represent the means and vertical lines the standard deviations; dots represent predicted temperatures. Datasets (setpoint temperatures) for *isobutanol* (INN R5): (a) 15.0 °C; (b) 21.0 °C.

Fig. 8

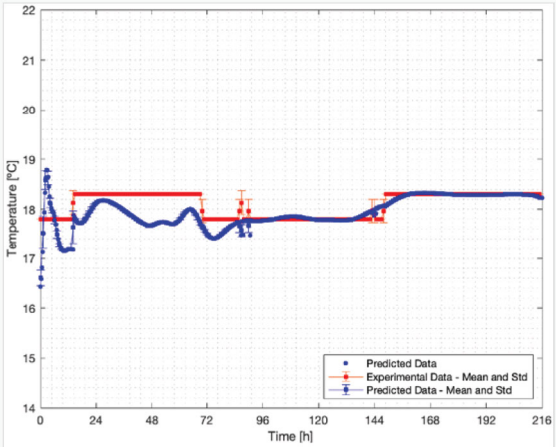

Ethyl acetate, Temp 19 °C (**a**)

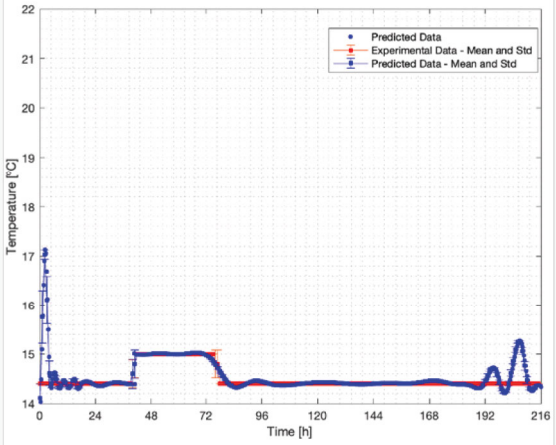

Amyl alcohols, Temp 15.0 °C (**b**)

Graphs of the experimental temperature values of two of the worst data sets. In red the experimental data measured by the sensor; in blue the predictions made by the inverse neural networks. The squares represent the means and the vertical lines the standard deviations; the dots represent forecast temperatures. Datasets for: (a) *ethyl acetate* 19.0 °C; (b) *amyl alcohols* 15.0 °C.

Table 4 presents a statistical comparison between the experimental temperatures from datasets (1–5) obtained in a previous study (Moya-Almeida et al., 2021) and the temperatures simulated by the INNs, excluding the data from the initial 24 h of fermentation. The table includes the means, standard deviation, coefficients of determination, and the *F* and *p* values results from the analysis of variance.

alt-text: Table 4

Table 4

The table layout displayed in this section is not how it will appear in the final version. The representation below is solely purposed for providing corrections to the table. To view the actual presentation of the table, please click on the Preview located at the top of the page.

Statistics for the goodness of fit of inverse neural network models.

Compounds		R	R^2	MSE
isobutanol (R5)	Training (75 %)	0.991	0.982	0.069
	Testing (25 %)	0.992	0.984	0.062
	Total (100 %)	0,991	0982	
ethyl acetate (R6)	Training (75 %)	0.991	0.982	0.070
	Testing (25 %)	0.988	0.976	0.084
	Total (100 %)	0,991	0982	
amyl alcohols (R7)	Training (75 %)	0.993	0.986	0.053
	Testing (25 %)	0.995	0.990	0.041
	Total (100 %)	0,993	0986	
n-propanol (R8)	Training (75 %)	0.993	0.986	0.049
	Testing (25 %)	0.988	0.976	0.086
	Total (100 %)	0,992	0984	

Abbreviations. (R) Correlation coefficient. (R^2) Coefficient of determination. (MSE) mean squared error.

For 15 out of the 20 cases studied, p-values greater than 0.05 indicates that there are no statistically significant differences between the two datasets. However, in the cases referring to *ethyl acetate* for temperatures of 18 and 19 °C and *amyl alcohols* for 15.0, 16.5 and 18.0 °C, low determination coefficients are given, in addition to high *F* and very low *p* values that are interpreted as different datasets from each other. However, the means and standard deviations of these datasets demonstrate that they yield very similar data in terms of estimating the fermentation temperature for control purposes: *ethyl acetate* F3: 17.3–17.2 °C, F4: 18.0–18.1 °C; *amyl alcohols* F1: 14.6–14.5 °C, F2: 15.8–15.8 °C, F3: 17.2–17.2 °C; means temperature simulated and experimentally registered respectively. This phenomenon arises due to the consistent nature of the experimental values, whereas the simulated values exhibit temporal variability. However, when these values are averaged, they converge to a value very close to the experimental data (Fig. 8). In this work, the average of the simulated values is precisely the temperature setpoint utilized, thus the low coefficients of determination observed in the mentioned cases do not represent a difficulty. Conversely, optimal results are achieved in all other instances.

4.3 Experimental work: validation of the INNs and the fuzzy controller

To validate the performance of the proposed method, the solvent concentrations specified in Table 1 were inputted into the four INNs (R5 for *isobutanol*, R6 for *ethyl acetate*, R7 for *amyl alcohols*, and R8 for *n-propanol*). For each batch, four simulated temperatures were obtained, with one corresponding to each compound. These four values were then averaged to obtain a single target temperature. However, it should be noted that although four temperature setpoints are calculated, the fermenter can only manage one. The procedure was repeated for each of the four fermentations

conducted (F1 – F4). The temperature setpoints obtained are for F1: 15.53 °C, for F2: 16.84 °C, for F3: 17.81 °C, and for F4: 18.87 °C. Table 5 shows the temperatures calculated by the INNs and their statistical data. Subsequently, the fuzzy controller utilized these setpoint temperatures.

alt-text: Table 5

Table 5

Statistical comparison of the temperatures simulated by the INNs against experimental data. The *F* and *p* statistics are the result of the analysis of variance.

Datasets (Temp °C)	Compounds	Simulated vs experimental temperatures			Means °C		Standard Deviation °C	
		F *	*p*	R^2	Simulated	Experimental	Simulated	Experimental
1 (15.0)	*isobutanol*	1.0652	0.4490	0.9695	14.5	14.5	0.24	0.24
2 (16.5)		1.0197	0.8151	0.9832	15.8	15.8	0.27	0.27
3 (18.0)		1.1038	0.2366	0.9298	17.2	17.2	0.22	0.21
4 (19.0)		0.9617	0.6394	0.9837	18.1	18.1	0.24	0.24
5 (21.0)		1.0508	0.5525	0.9585	20.0	20.0	0.14	0.14
1 (15.0)	*ethyl acetate*	0.9921	0.9245	0.9948	14.5	14.5	0.23	0.24
2 (16.5)		0.9716	0.7302	0.9918	15.8	15.8	0.26	0.27
3 (18.0)		2.0018	1.77×10^{-16}	0.2794	17.3	17.2	0.30	0.21
4 (19.0)		1.1495	0.0951	0.0876	18.0	18.1	0.26	0.24
5 (21.0)		1.0285	0.7367	0.8428	20.0	20.0	0.14	0.14
1 (15.0)	*amyl alcohols*	1.4192	2.85×10^{-05}	0.4343	14.6	14.5	0.28	0.24
2 (16.5)		1.5027	1.15×10^{-06}	0.3697	15.8	15.8	0.33	0.27
3 (18.0)		0.7629	0.0012	0.7820	17.2	17.2	0.18	0.21
4 (19.0)		1.1328	0.1353	0.9551	18.1	18.1	0.26	0.24
5 (21.0)		0.9661	0.6795	0.8956	20.0	20.0	0.13	0.14
1 (15.0)	*n-propanol*	0.9986	0.9865	0.9979	14.5	14.5	0.24	0.24
2 (16.5)		1.0290	0.7319	0.9980	15.8	15.8	0.27	0.27
3 (18.0)		1.0791	0.3617	0.9830	17.2	17.2	0.22	0.21
4 (19.0)		0.9925	0.9278	0.9901	18.1	18.1	0.24	0.24
5 (21.0)		1.0049	0.9534	0.9916	20.0	20.0	0.14	0.14

* The table value of *F* (p = 0.05) for all cases is 1.1472.

We observe the highest variabilities in ethyl acetate (F1 = 0.835, F2 = 1.129, F3 = 0.752, F4 = 0.543). This aligns with the fact that the corresponding INNs for this compound exhibit low coefficients of determination (R^2 = 0.279, R^2 = 0.088), as shown in Table 5. A similar effect occurs with amyl alcohols, which demonstrate higher standard deviations for three of their datasets (F1 = 1.021, F2 = 0.684, F3 = 0.542), while the coefficients of determination for their respective inverse neural networks, in the same aforementioned case, exhibit values of (R^2 = 0.434, R^2 = 0.370,

$R^2 = 0.782$). However, it is also evident that when averaging the obtained results, the impact of these distortions on the outcome tends to diminish.

Using the setpoint temperatures determined by the inverse neural networks (INNs), a total of four fermentations were conducted.

Regarding temperature, real-world scenarios show that temperature values exhibit temporal variations during the fermentation process. Therefore, Table 6 provides statistical data for these measurements recorded by the Tilt sensor.

alt-text: Table 6

Table 6

Statistical data of simulated temperatures obtained by INNs models.

Datasets	Compounds	Max	Min	Mean	SD	Setpoint temperatures	Error[a]
F1	*n-propanol*	17.20	15.45	15.78	0.348	15.53	−0.25
F2		17.63	16.43	16.68	0.221	16.84	0.16
F3		18.09	17.41	17.66	0.156	17.81	0.15
F4		19.41	16.92	18.90	0.422	18.87	−0.03
F1	*ethyl acetate*	18.65	12.02	15.45	0.835	15.53	0.08
F2		19.97	15.89	16.96	1.129	16.84	−0.12
F3		20.03	17.51	18.18	0.752	17.81	−0.37
F4		19.99	18.13	19.04	0.543	18.87	−0.17
F1	*amyl alcohols*	17.19	12.05	15.45	1.021	15.53	0.08
F2		17.23	15.06	16.36	0.684	16.84	0.48
F3		19.56	17.42	17.86	0.542	17.81	−0.05
F4		19.40	18.54	18.88	0.212	18.87	−0.01
F1	*isobutanol*	16.76	14.66	15.45	0.364	15.53	0.08
F2		18.12	16.07	17.35	0.542	16.84	−0.51
F3		18.24	17.08	17.55	0.305	17.81	0.26
F4		19.38	18.23	18.66	0.338	18.87	0.21

All values are given in °C.
Abbreviations: standard deviation (SD).

Table Footnotes

[a] Difference between the setpoint and mean temperature.

As an example, Fig. 9 illustrates the time series of temperature data recorded, along with the fermentation temperature setpoint for F3. The records for F1, F2, and F4 exhibit similar characteristics.

alt-text: Fig. 9

Fig. 9

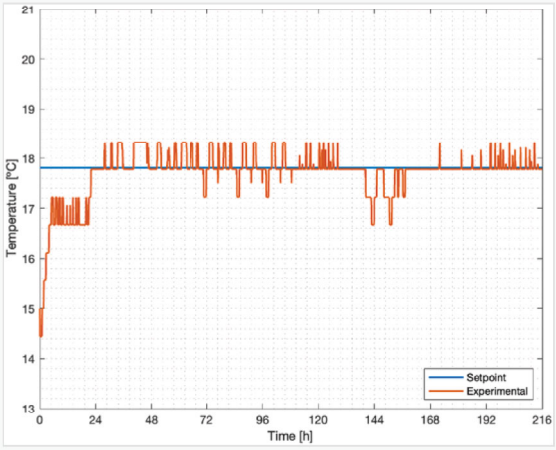

Temperature values recorded along time by the Tilt sensor (red line) versus the setpoint temperature for fermentation F3 (blue line).

Moreover, daily samples were collected and subsequently analyzed using GC-FID to measure the concentrations of each compound. The results indicate that the final concentrations closely align with the target concentrations specified in Table 1. For further analysis, Table 8 provides a detailed overview of the average concentrations obtained during the last three days of each compound for all four fermentations.

alt-text: Table 8

Table 8

The table layout displayed in this section is not how it will appear in the final version. The representation below is solely purposed for providing corrections to the table. To view the actual presentation of the table, please click on the Preview located at the top of the page.

The average concentration in $mg \cdot L^{-1}$ of the last three days of the fermentation process for each compound and fermentation carried out.

Compound	Fermentation	Setpoint [a]	Day 7 [b]	Day 8 [b]	Day 9 [b]	Mean [c]	SD [d]	E [e]
isobutanol	F1	24.40	25.24	24.39	24.57	24.73	0.531	−0.33
	F2	30.00	29.41	29.36	29.28	29.35	0.646	0.65
	F3	39.50	40.31	39.23	40.32	39.95	0.906	−0.40
	F4	44.00	43.07	42.99	44.32	43.46	0.999	0.54
ethyl acetate	F1	22.50	22.09	22.52	22.49	22.37	0.456	0.13
	F2	25.75	25.49	25.47	25.49	25.48	0.627	0.27
	F3	27.15	28.47	27.10	27.47	27.68	0.923	−0.53
	F4	28.15	28.12	28.17	28.30	28.20	0.610	−0.05

amyl alcohols	F1	59.12	59.25	58.60	59.43	59.09	1.936	0.03
	F2	63.00	63.04	62.46	63.06	62.85	0.949	0.15
	F3	67.50	70.11	68.25	69.10	69.15	1.384	−1.65
	F4	72.80	71.76	70.73	71.38	71.29	1.522	1.51
n-propanol	F1	23.35	23.36	23.30	23.37	23.34	0.172	0.01
	F2	24.50	24.26	24.32	24.34	24.31	0.187	0.19
	F3	25.85	25.41	25.61	25.74	25.59	0.323	0.26
	F4	27.10	27.12	27.27	27.67	27.35	1.222	−0.25

Table Footnotes

[a] Concentration' setpoint. Values are taken from Table 1.

[b] Mean values of the three daily measurements taken.

[c] Average of the means of the last three days.

[d] Standard deviation of all measurements taken during the last three days of the fermentations.

[e] Error. Difference between setpoint and the average of the means value. Negative values represent that the concentrations obtained are greater than the setpoint, and positive values represent the opposite.

Figs. 10–13 depict the time evolution of the final concentrations for each compound concerning the four selected target concentrations (Table 1).

alt-text: Fig. 10

Fig. 10

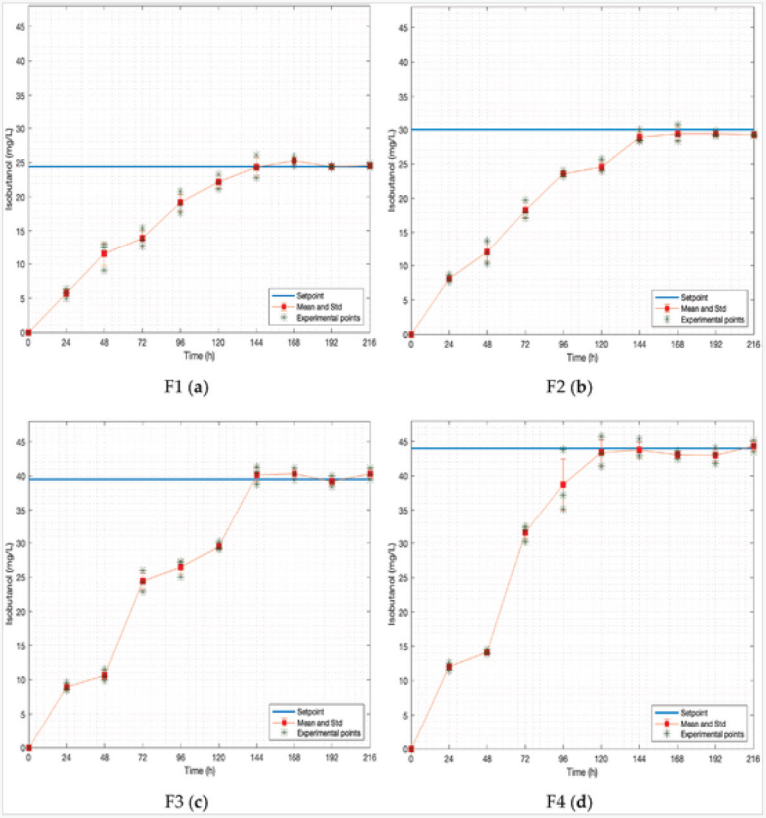

Evolution of *isobutanol* through 216 h concerning the setpoint as the final concentration of the compound, over the four fermentations: (**a**) F1: 24.40 mg L^{-1}; (**b**) F2: 30.00 mg L^{-1}; (**c**) F3: 39.50 mg L^{-1}; (**d**) F4: 44.00 mg L^{-1}.

alt-text: Fig. 11

Fig. 11

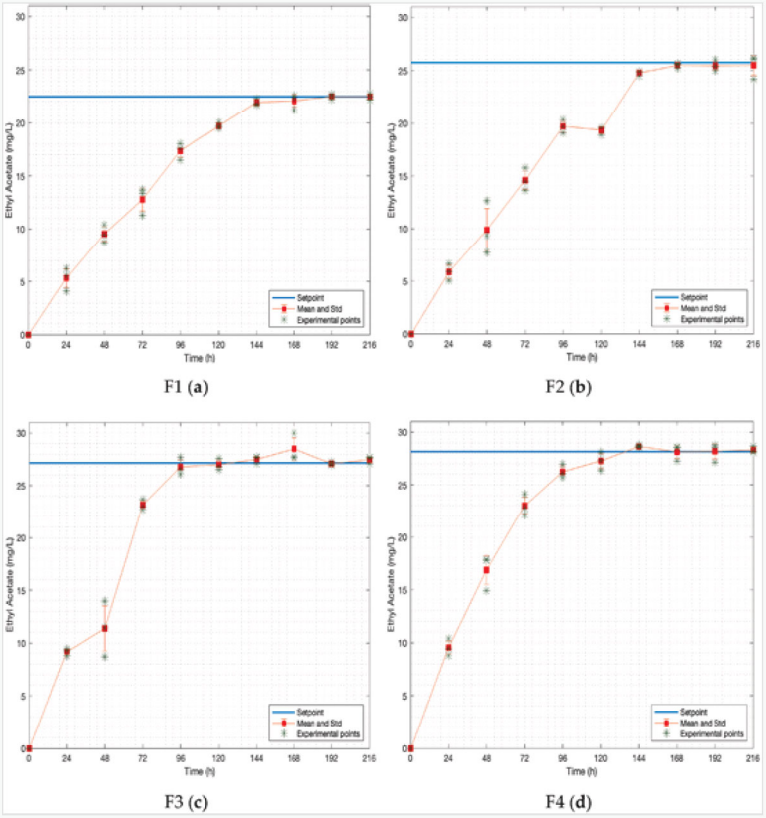

Evolution of *ethyl acetate* through 216 h concerning the setpoint of the final concentration of the compound, over the four fermentations: **(a)** F1: 22.50 mg L^{-1}; **(b)** F2: 25.75 mg L^{-1}; **(c)** F3: 27.15 mg L^{-1}; **(d)** F4: 28.15 mg L^{-1}.

alt-text: Fig. 12

Fig. 12

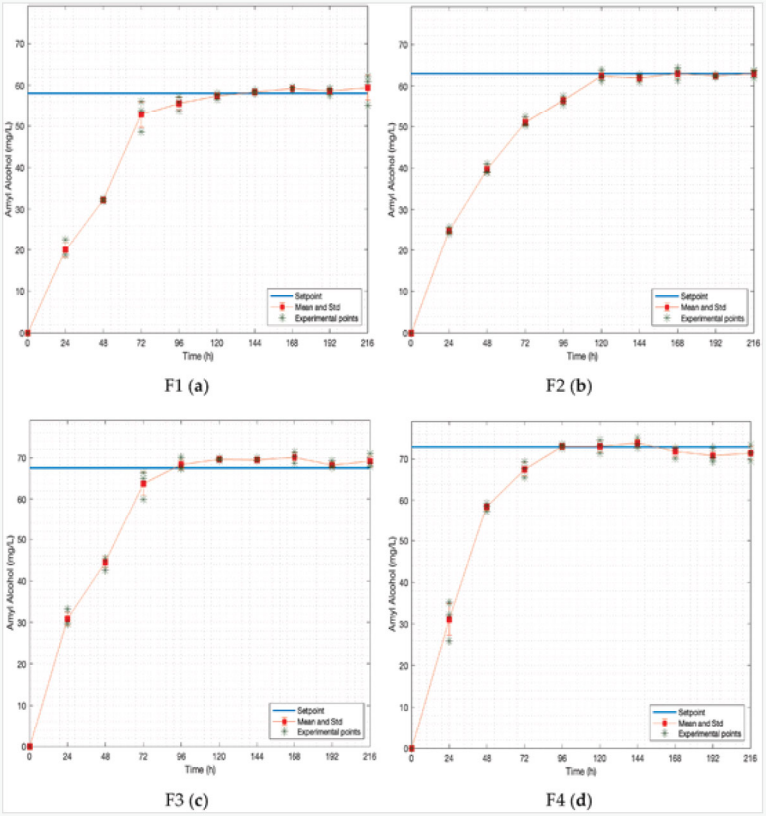

Evolution of *amyl alcohol* through 216 h concerning the setpoint of the final concentration of the compound, over the four fermentations: **(a)** F1: 59.12 mg L^{-1}; **(b)** F2: 63.00 mg L^{-1}; **(c)** F3: 67.50 mg L^{-1}; **(d)** F4: 72.80 mg L^{-1}.

alt-text: Fig. 13

Fig. 13

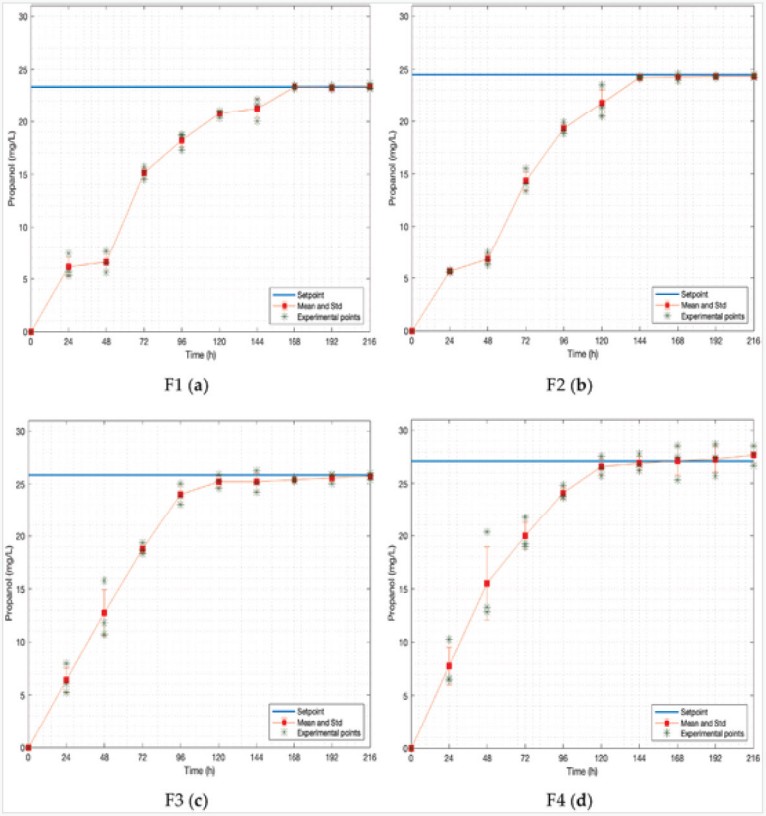

Evolution of *propanol* through 216 h concerning the setpoint of the final concentration of the compound, over the four fermentations: (**a**) F1: 23.35 mg L^{-1}; (**b**) F2: 24.50 mg L^{-1}; (**c**) F3: 25.85 mg L^{-1}; (**d**) F4: 27.10 mg L^{-1}.

In the case of *n-propanol*, the fermentation (F1) achieved the value closest to the setpoint, E = 0.01 mg L^{-1}, among all the conducted fermentations. Overall, *n-propanol* exhibited the most favourable outcomes. The only unsuitable result was the standard deviation of the F4, SD = 1.22, which is the third-worst record of all the datasets.

The two most unfavourable results, E = −1.65 mg L^{-1} (F3) and E = 1.51 mg L^{-1} (F4), were observed in *amyl alcohols*, and they also exhibited the highest standard deviations, SD = 1.936 (F1), SD = 1.384 (F3), and SD = 1.522 (F4). This could be attributed to the fact that *amyl alcohols* represent a group of chemical compounds rather than a single entity.

In the same order of ideas, if we compare the $\overline{TE}$, which is observed in Table 7, in three cases (F1 – F3) we obtain a positive value, which means that the temperatures remain below the setpoint, while in F4 it is the opposite. The errors are relatively small if we compare them with the order of magnitude of the temperatures (max0.27 °C).

alt-text: Table 7

Table 7

The table layout displayed in this section is not how it will appear in the final version. The representation below is solely purposed for providing corrections to the table. To view the actual presentation of the table, please click on the Preview located at the top of the page.

Statistics of the temperature °C data recorded by the Tilt sensor.

Fermentation datasets	Setpoint	Mean	Min	Max	SD	$\overline{TE}$ [a]
F1	15.53	15.26	13.3	17.2	0.556	0.27

F2	16.84	16.59	14.4	17.2	0.307	0.25
F3	17.81	17.69	14.4	18.3	0.503	0.12
F4	18.87	19.13	15.6	20.0	0.619	−0.26

Abbreviations: standard deviation (SD).

Table Footnotes

[a] Mean Temperature Error. Difference between setpoint and mean temperature. Negative values represent that the temperature is greater than the setpoint, and positive values represent the opposite.

By combining fuzzy logic with INNs, it has been feasible to achieve solvent concentrations that closely align with the setpoint values designated by an expert user.

5 Conclusions

To the best of the authors' knowledge, this is the first study that predicts the optimal temperature necessary to achieve expert-designated concentrations of a set of solvent compounds (*isobutanol*, *n-propanol*, *amyl alcohol*, *ethyl acetate*) produced by the yeast *S. cerevisiae* Safale S04 during the alcoholic fermentation process.

The study has demonstrated the remarkable accuracy of inverse neural networks in predicting the temperatures required to achieve user-specified final concentrations, using experimental data such as real-time temperature and time for their operation, as well as compound measurements for their training. Additionally, the incorporation of fuzzy controllers offers significant advantages, including flexibility, ease of use, and reduced work time, as they primarily rely on expert knowledge rather than the intricate development of mathematical models, which can be complex in fields such as fermentation.

The concentration of *n-propanol* achieved exhibited the highest level of accuracy, with an average error of 0.18 mg L^{-1}. Conversely, the final concentration of *amyl alcohols* yielded the least precise results, with an average error of 0.83 mg L^{-1}. Nevertheless, it can be considered that this value is relatively low when compared to the magnitude of the concentrations of the compounds under study.

The utilization of neural networks and fuzzy controllers demonstrates significant potential in enhancing the final organoleptic characteristics of beers, which, to the best of the authors' knowledge, is a relatively unexplored application of these tools.

In practical terms, it is expected that this technique can be replicated for other compounds, microorganisms, brewing styles, beer production methods, different ingredient combinations, other alcoholic beverages such as wine or cider, and even with other types of fermentations such as acetic or lactic fermentation. All of this is aimed at producing beverages with predetermined quantities of compounds, as specified by expert users.

Funding

This research was funded by Secretaría de Educación Superior, Ciencia, Tecnología e Innovación de la República de Ecuador: ARSEQ-BEC-005319-2016.

CRediT authorship contribution statement

Vinicio Moya-Almeida : Conceptualization, Methodology, Software, Validation, Formal analysis, Investigation, Resources, Visualization, Writing – original draft, Funding acquisition, Data curation, Writing – review & editing. **Belén Diezma-Iglesias :** Conceptualization, Resources, Visualization, Writing – original draft, Writing – review & editing, Supervision. **Eva Cristina-Correa :** Conceptualization, Resources, Visualization, Writing – original draft, Writing – review & editing, Supervision.

Declaration of competing interest

The authors declare the following financial interests/personal relationships which may be considered as potential competing interests: Vinicio Moya Almeida reports financial support was provided by Secretaría de Educación Superior, Ciencia, Tecnología e Innovación de la República de Ecuador.

Acknowledgements:

The authors would like to express their gratitude to the Chemistry and Food Technology Department of the Universidad Politécnica de Madrid (UPM) for their invaluable technical support in conducting gas chromatography analysis.

References

The corrections made in this section will be reviewed and approved by a journal production editor. The newly added/removed references and its citations will be reordered and rearranged by the production team.

Averill, A.F., 2020. The usefulness and application of fuzzy logic and fuzzy AHP in the materials finishing industry. Trans. Inst. Met. Finish. 98 (5), 224–233. doi:10.1080/00202967.2020.1802082.

Birle, S., Hussein, M.A., Becker, T., 2015. On-line yeast propagation process monitoring and control using an intelligent automatic control system. Eng. Life Sci. 15 (1), 83–95. doi:10.1002/elsc.201400058.

BJCP, 2015. 2015 Style Guidelines. https://www.bjcp.org/docs/2015_Guidelines_Beer.pdf.

BJCP, 2021a. 2021 Style Guidelines. https://www.bjcp.org/bjcp-style-guidelines/.

BJCP, 2021b. Beer Faults. https://dev.bjcp.org/education-training/education-resources/beer-faults/.

Carrillo-Ureta, G.E., Roberts, P.D., Becerra, V.M., 2001. Genetic Algorithms for Optimal Control of Beer Fermentation. pp. 391–396. doi:10.1109/ISIC.2001.971541.

Gonzalez Viejo, C., Torrico, D.D., Dunshea, F.R., Fuentes, S., 2019. Development of artificial neural network models to assess beer acceptability based on sensory properties using a robotic pourer: a comparative model approach to achieve an artificial intelligence system. Beverages (Basel) 5 (2), 33. doi:10.3390/beverages5020033.

Huang, Y., Kangas, L.J., Rasco, B.A., 2007. Applications of artificial neural networks (ANNs) in food science. Crit. Rev. Food Sci. Nutr. 47 (2), 113–126. doi:10.1080/10408390600626453.

Humia, B.V., Santos, K.S., Barbosa, A.M., Sawata, M., Mendonça, M.d.C., Padilha, F.F., 2019. Beer molecules and its sensory and biological properties: a review. Molecules 24 (8), 1568.

doi:10.3390/molecules24081568.

Imtiaz, U., Assadzadeh, A., Jamuar, S.S., Sahu, J.N., 2013. Bioreactor temperature profile controller using inverse neural network (INN) for production of ethanol. J. Process Control 23 (5), 731–742. doi:10.1016/j.jprocont.2013.03.005.

Kunze, W., Hendel, O., 2019. Technology Brewing and Malting. 6th English ed. VLB Berlin, Berlin Retrieved from http://d-nb.info/1188741039/04.

Li, D., Qian, L., Jin, Q., Tan, T., 2011. Reinforcement learning control with adaptive gain for a saccharomyces cerevisiae fermentation process. Appl. Soft Comput. 11 (8), 4488–4495. doi:10.1016/j.asoc.2011.08.022.

Loira, I., Vejarano, R., Morata, A., Ricardo-da-Silva, J.M., Laureano, O., González, M.C., Suárez-Lepe, J.A., 2013. Effect of saccharomyces strains on the quality of red wines aged on lees. Food Chem. 139 (1), 1044–1051. doi:10.1016/j.foodchem.2013.01.020.

Loviso, C.L., Libkind, D., 2018. Synthesis and regulation of flavor compounds derived from brewing yeast: esters. Rev. Argent. Microbiol. 50 (4), 436–446. doi:10.1016/j.ram.2017.11.006.

Loviso, C.L., Libkind, D., 2019. Synthesis and regulation of flavor compounds derived from brewing yeast: fusel alcohols. [Sintesis y regulacion de los compuestos del aroma y sabor derivados de la levadura en la cerveza: alcoholes superiores. Rev. Argent. Microbiol.. doi:10.1016/j.ram.2018.08.006.

Martinez, G., López, A., Esnoz, A., Virseda, P., Ibarrola, J., 1999. A new fuzzy control system for white wine fermentation. Food Control 10 (3), 175–180. doi:10.1016/S0956-7135(99)00015-8.

Martins, C., Brandão, T., Almeida, A., Rocha, S.M., 2020. Enlarging knowledge on lager beer volatile metabolites using multidimensional gas chromatography. Foods 9 (9), 1276. doi:10.3390/foods9091276.

Medl, M., Rajamanickam, V., Striedner, G., Newton, J., 2023. Development and validation of an artificial neural-network-based optical density soft sensor for a high-throughput fermentation system. Processes 11 (1), 297. doi:10.3390/pr11010297.

Meilgaard, M.C., Dalgliesh, C.E., Clapperton, J.F., 1979. Beer flavor terminology. J. Inst. Brew. 85 (1), 38–42. doi:10.1002/j.2050-0416.1979.tb06826.x.

Moya-Almeida, V., Diezma Iglesias, B., Correa Hernando, E.C., 2021. Artificial neural networks and gompertz functions for modelling and prediction of solvents produced by the S. cerevisiae safale S04 yeast. Fermentation 7 (4), 217. doi:10.3390/fermentation7040217.

Nelson, D.L., Cox, M.M., Hoskins, A.A., 2021. In: Freeman, W.H. (Ed.), Lehninger Principles of Biochemestry, eighth ed. MPS, New York, USA.

Oliver, G., 2013. The Oxford Companion to Beer. Oxford University Press, New York Retrieved from doi:10.1093/acref/9780195367133.001.0001. https://www.oxfordreference.com/view/10.1093/acref/9780195367133.001.0001/acref-9780195367133.

Oussalah, M., Nguyen, H.T., Kreinovich, V., 2001. A new derivation of centroid defuzzification. Paper presented at the 10th IEEE International Conference on Fuzzy Systems. (*Cat.* no.01CH37297) Melbourne, VIC, Australia 2 884-887 vol.3 https://ieeexplore.ieee.org/document/1009097.

Pedrycz, W., 2021. An Introduction to Computing with Fuzzy Sets: Analysis, Design, and Applications. first ed. Springer International Publishing, Switzerland Retrieved from doi:10.1007/978-3-030-52800-3. https://lin

k.springer.com/book/10.1007/978-3-030-52800-3.

Rodrigues, F.R., Erni, S.J., Frattini Fileti, A.M., Vasconcelos, d.S.F., 2013. A fuzzy-split range control system applied to a fermentation process. Bioresour. Technol. 142, 475–482. doi:10.1016/j.biortech.2013.05.083.

Sipos, A., Florea, A., Arsin, M., Fiore, U., 2021. Using neural networks to obtain indirect information about the state variables in an alcoholic fermentation process. Processes 9 (1). doi:10.3390/pr9010074.

Smogrovicova, D., Domeny, Z., 1999. Beer volatile by-product formation at different fermentation temperature using immobilised yeasts. Process Biochem. 34 (8), 785–794. doi:10.1016/S0032-9592(98)00154-X.

Sousa, B.S., Silva, F.V., Fileti, A.M.F., 2019. Level control of coupled tank system based on neural network techniques. Chem. Prod. Process Model. 15 (3), 540. doi:10.1515/cppm-2019-0086.

Syu, M., Tsao, G., Austin, G., Celotto, G., D'Amore, T., 1994. Neural-network modeling for predicting brewing fermentations. J. Am. Soc. Brew. Chem. 52 (1), 15–19. doi:10.1094/ASBCJ-52-0015.

Venkateswarlu, C., Gangiah, K., 1995. Fuzzy modeling and control of batch beer fermentation. Chem. Eng. Commun. 138 (1), 89–111. doi:10.1080/00986449508936383.

Verstrepen, K.J., Derdelinckx, G., Dufour, J.P., Winderickx, J., Thevelein, J.M., Pretorius, I.S., Delvaux, F.R., 2003. Flavor-active esters: adding fruitiness to beer. J. Biosci. Bioeng. 96 (2), 110–118. doi:10.1016/S1389-1723(03)90112-5.

Villacreces, S., Blanco, C., Caballero, I., 2022. Developments and characteristics of craft beer production processes. Food Biosci. 45, 101495. doi:10.1016/j.fbio.2021.101495.

Wang, B., Ji, X.F., Zhuang, Z.K., 2015. Soft-sensing modeling based on PSO-FNN inversion for penicillin fermentation process. Chemical Engineering Transactions 46, 1333–1338. doi:10.3303/CET1546223.

Wang, X., Liu, C., Song, Z., Wu, B., 2015. In: Improved Variable Universe Fuzzy PID Application in Beer Fermentation Process. Paper Presented at the 2015 International Conference on Machine Learning and Cybernetics (ICMLC), vol. 1. pp. 40–46 Guangzhou, China doi:10.1109/ICMLC.2015.7340895. https://ieeexplore.ieee.org/document/7340895.

White, C., Zainasheff, J., 2010. Yeast: the Practical Guide to Beer Fermentation. Brewers Publications, Portland. https://www.brewerspublications.com/products/yeast-the-practical-guide-to-beer-fermentation.

Xu, G., Liu, J., 2007. Research of temperature characteristics and control algorithm in the beer fermentation process. In: Paper Presented at the *2nd* IEEE Conference on Industrial Electronics and Applications. pp. 192–194 Harbin, China doi:10.1109/ICIEA.2007.4318397. https://ieeexplore.ieee.org/document/4318397.

Xu, X.Q., 2013. Beer fermentation temperature control curve optimization based on the fuzzy - neural network PID control algorithm. In: Paper Presented at the International Conference on Mechatronics and Semiconductor Materials. ICMSCM 2013 846-847(Advanced Materials Research) 325-328 doi:10.4028/www.scientific.net/amr.846-847.325. https://www.scientific.net/AMR.846-847.325.

Zadeh, L.A., 1965. Fuzzy sets. Inf. Control 8 (3), 338–353. doi:10.1016/S0019-9958(65)90241-X.

Zhang, R., 2018. On-line monitoring of ethanol concentration during biomass fermentation. Proc. 2018 Int. Conf. Mech. Electr. Control and Autom. Eng. (Mecae 2018) 149, 395–399. doi:10.2991/mecae-18.2018.77.

Zhang, Y., Jia, S., Zhang, W., 2013. Predicting acetic acid content in the final beer using neural networks and support vector machine. J. Inst. Brew. 118 (4), 361–367. doi:10.1002/jib.50.

Zhu, X.L., Jiang, Z.Y., Wang, B., He, Y.J., 2018. Decoupling control based on fuzzy neural-network inverse system in marine biological enzyme fermentation process. IEEE Access 6, 36168–36175. doi:10.1109/ACCESS.2018.2842181.

Graphical abstract

Images may appear blurred during proofing as they have been optimized for fast web viewing. A high quality version

alt-text: Image 1